Magnetization Process and Interlayer Coupling in MnNi/Co/Ag(Cu)/Py High-Temperature Annealed Spin Valves

N. A. Tuan[*], L. V. Su, T. T. Hoai Dung, N. A. Tue, H. Q. Khanh

Hanoi University of Science and Technology - No. 1, Dai Co Viet, Hai Ba Trung, Hanoi, Viet Nam
Received: April 06, 2019; Accepted: November 28, 2019

Abstract

MnNi/Co/Ag/Py and MnNi/Co/Cu/Py spin valves, where Py is the symbol for permalloy $Ni_{81}Fe_{19}$, were prepared using magnetron sputtering followed by a high temperature annealing at T_a = 300°C and 400°C for 30 minutes in high vacuum (~10^{-5} torr). The magnetization process and the magnetic coupling between ferromagnetic layers of these spin valves were investigated. The results show a weak magnetic coupling behavior, moreover, a weak positive exchange bias coupling between Co and Py layers, and a trend of an out-of-plane magnetic anisotropy in these spin valves. The origin of these features or behaviors are discussed in detailed. These results will be useful information for technological adjustments to achieve the expected properties for magnetic coupling and magnetic anisotropy of the spin valve devices.

Keywords: Spin valve, magnetization process, magnetic coupling, out-of-plane anisotropy, positive exchange biased coupling

1. Introduction

Spin valve (SV) is used to control the spin polarized current through the spin dependent scattering mechanism which is manifested as giant magnetoresistance (GMR) effect. A relative arrangement in magnetization (M) directions between two ferromagnetic layers (FM) separated by a non-magnetic (NM) layer in the SV can be controlled by an external magnetic field, H [1,2]. Largest spin current, corresponding to a lowest resistance, can be achieved when the M directions are in a parallel arrangement, and a smallest spin current, hence highest resistance, when these M directions are aligned completely antiparallel. To make the control more easily for the SV, one of the two FM layers is usually pinned by an antiferromagnetic (AFM) layer, while the other is free. The SVs have been used extensively in modern magnetic devices of the next generation – *spintronics* [3-5].

Magnetization process reflects the relative arrangement in the M directions and magnetic coupling between two FM layers in the SVs. Therefore, toward manufacturing and studying SVs, the investigation of the magnetization process and the coupling between the FM layers of the SV is a necessary demand. Two different SV systems of NM layers, corresponding to Ag and Cu in the MnNi/Co/Ag/Py and MnNi/Co/Cu/Py structures

(Fig.1a), were investigated. Here, the MnNi AFM layer acts as a pinning layer to pin the Co layer, whereas the Py layer acts as a free one. On the other hand, by using the rather thick thicknesses of the Ag and Cu layers, such as 6 nm and 12 nm, we perfomed a non-coupling- (or weak-coupling-) type SV structure. For such SV structures, interlayer magnetic coupling is an unnecessary condition but magnetic structural changes by any reason may also cause an GMR effect and this effect can be exhibited in very weak magnetic fields [6]. To help understand the mechanism of the spin dependent magnetic transport in our upcoming study, in this paper, we investigate just on the process of magnetization reverse and magnetic coupling for the SVs annealed at high temperatures.
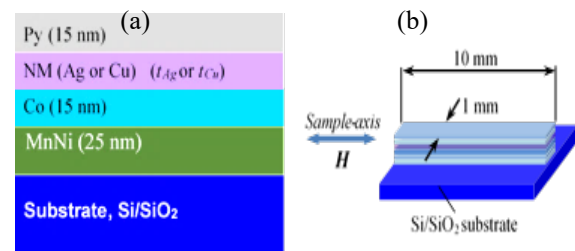

Fig. 1. (a) Cross-section of the MnNi/Co/Ag(Cu)/Py SV structures. (b) Experimental setup for hysteresis-loop measurements of an in-plane configuration.

[*] Corresponding author: Tel.: (+84) 966.618.777
Email: natuan.itims@hust.edu.vn

2. Experimental

MnNi/Co/Ag(Cu)/Py SVs (Fig.1a), where MnNi and Py (permalloy) are $Mn_{50}Ni_{50}$ and $Ni_{81}Fe_{19}$ alloys, respectively, were deposited on the Si(100)/SiO$_2$ substrates using *rf* sputtering with a power of 300W, base vacuum of lower than ~10^{-6} mbar and argon pressure of ~ 10^{-3} mbar for sputtering. 3-inch targets of MnNi-alloy, Py-alloy, Co, Ag and Cu were used. The deposition process of the MnNi, Py, Co, Ag and Cu thin films that correspond to the layers of MnNi/Co/Ag(Cu)/Py is sequentially as follows. Firstly, a 25-nm-MnNi layer is deposited on the Si(100)/SiO$_2$ substrate, later a 15-nm-Co layer is superposed on. Then, an Ag (or Cu) layer with various thicknesses t_{Ag} (or t_{Cu}) of 6 nm and 12 nm are deposited on top of the previously covered MnNi/Co layers. Finally, a 15-nm-Py cap layer is deposited on top of the Ag (or Cu) layer. Deposition parameters R, determinated experimentally corres-ponding to each layer through thicknesses investigations (Alpha-step IQ from KLAT-Tencor corporation) for a given depositing time, respectively are about 3 nm/min for MnNi, 1.7 nm/min for Co, 7.2 nm/min for Ag, 3.5 nm/min for Cu, and 1.8 nm/min for Py. Based on these data, nominal thicknesses determined corresponding to each layer, respectively are t_{MnNi} = 25 nm, t_{Co} = t_{Py} = 15 nm, t_{Ag} (and t_{Cu}) = 6 and 12 nm. Here, the SV samples will be called under the symbols SV1 and SV2 for the samples with the Ag layer of 6-nm and 12-nm thickness, and SV3 and SV4 corresponding with the Cu layer of 6-nm and 12-nm thickness. A Si mask with the 1 mm-width and 10 mm-length slits for forming the 1×10 mm^2-rectangular-bar samples was used. The samples were treated by subsequent annealing in vacuum ~10^{-5} mbar for 0.5 hour at various temperatures, from 100°C to 500°C. Magnetization process were investigated using a vibrating sample magnetometer with a H applied parallel to the film plane, i.e. along the sample-axis (see Fig.1b). As mentioned, only samples annealed at T_a = 300°C and 400°C are considered and analyzed here.

3. Results and disscution

Magnetic properties of all the samples as a function of t_{Ag}, t_{Cu}, and T_a have shown that, basically, t- and T_a-dependent behaviors in magnetic coupling (not presented here) are like common behaviors reported in other studies. For instance, that were of oscillatory behavior beween FM-type and AFM-type coupling in a system including FM layers separated by NM metal spacers, or phenomena related to changes in coercive force H_C [1,7-10]. However, some remarkable points in magnetization process and magnetic coupling of these high-T_a SVs can be summaied as follows.

Firstly, as seen in Figs.2 and 3, in-plane $M(H)$ hysteresis loops of two SV sample systems showed some common and dominant features in magnetic properties of both these SV systems. This is a typical leaf-shape feature, or cusplike, of the hysteresis loops. These features seem to prove that a non-coupling or very weak coupled behaviour, which implied a rather random orientation between the magnetizations in the Py and Co layers, are quite suitable for 6- and 12-nm-thick Ag(Cu) layers. On the other hand, due to the Py layer behaves as a very soft magnet, the magnetizations in two Py and Co layers could be easily oriented antiparallely in a certain intensity range of external magnetic field. In other words, allthough presenting a non-coupling or very weak-coupling behaviour, the in-plane $M(H)$ loops still indicate a dominant tendency in a weak AFM-type coupling rather than strong AFM-type or FM-type coupling (Fig.4 expresses the AFM- and FM-type alignments of the magnetization coupling). Depending on t_{Ag}, t_{Cu} and T_a, leaf-shape loops that tend to be more upright can represent a FM-type coupling. Such typical cases can see in Fig.2c, d and f, or Fig.3c-f. Besides, a common tendency of out-of-plane anisotropy seems to be also indicated for the SVs, because a feature in a gentle slope in almost of the M(H) loops has been observed, as shown selectively in Fig.2a and 3a for the cases of the as-deposited samples. Note that, in these figures the original magnetization curves, which is indicated preliminaryly by illustrative strokes for describing, quite like a sign of measurements in the hard direction. As illustrated in Fig.4a, the case of the out-of-plane anisotropy will be expressed by a larger β altitude angle because of $|M_2'| < |M_2|$, while the case of the in-plane anisotropy corresponds with a smaller β due to $|M_2'| \approx |M_2|$. These arguments are based on suggestion that the Py layers are substantially in the in-plane anisotropy, but the Co layers have commonly the obvious out-of-plane anisotropy [11]. Furthermore, this out-of-plane anisotropy can be diminished considerably by a demagnetization field H_d induced significantly by the shape from the bar-form samples (Fig.4a). This means that the β altitude is considered as very small and $M_2' \equiv M_2$. The nature of the out-of-plane anisotropy of the Co layer is thought to originate basically from surface magnetic anisotropy, roughness of the interfaces and strains due to lattice mismatch between the substrate and the film [12,13]. As known, average anisotropy coefficient is $K_1 = K_b + 2K_s/t$, where t is ferromagnetic thickness, K_b and K_s are bulk and surface components, respectively. Thus, for a very thin Co film, a large perpendicular surface anisotropy makes the easy magnetization direction become perpendicular to the Co film plane. A recently published study on Co/CoO/Ag/Co sandwiches by us also has showed a rougher Ag/Co interface rather than Co/Ag interface [14]. This implies

that the Ag/Py interface (also similar to Cu/Py) in the MnNi/Co/Ag(Cu)/Py SVs can be quite rough in comparision with the Co/Ag interface, and thus can induce a magnetic surface anisotropy. This explains why the $M(H)$ loops of the SVs showed a quite faint FM-type alignment. A cusplike $M(H)$ loop can present a competition of first- and second-order uniaxial anisotropy components [15]. Another striking feature of the $M(H)$ loops is a two-step form, as seen in Fig.2a, d, Fig.3d, e, and faintly in other cases. This feature indicates a very weak interlayer coupling so that negligible in these SVs [6], and it can come from different H_C between Co and Py.

Secondly, for various materials used in the NM layers (Ag and Cu), generally, it can be also recognized easily an effective H_C was enhanced by utilizing Cu as the NM spacer layer (see values of H_C indicated in Fig.2 and 3). The enhancement in H_C can originate from an EBC consequence between the NiMn and Co layers, as ever proved in Ref. [10]. Notice that, the M behavior as a function of t_{Ag} and t_{Cu}, was expressed by a modification in shape of the $M(H)$ loops depending on t_{Ag} and t_{Cu}. This expression reflects a M

arrangement between the Py and Co layers. It proves that a M's alignment in the Py and Co layers changes between the FM- and AFM-types depending on t_{Ag} and t_{Cu}. Overall (not look in detail), the leaf-shape tendency with a quite bit gentler slope of the virgin curves of the loops (dashed lines shown in Fig.2a and Fig.3a), which indicated a more prominent AFM-type alignment, is more dominant in the thinner-t_{Ag} and SVs -t_{Cu} (t_{Ag} and t_{Cu} = 6 nm) than those in the thicker-t_{Ag} and -t_{Cu} SVs (t_{Ag} and t_{Cu} = 12 nm). Whereas, a bluffer manifestation of the $M(H)$ loops shows a more prominent FM-type alignment tendency for thicker-t_{Ag}'s and -t_{Cu}'s (compare overall the loops in Fig.2a-c and Fig.3a-c to the ones in Fig.2d, f and Fig.3d-f).

Next, considering the case of the effects of different high-T_a's on the magnetic properties of the SVs. Fig.2 and 3 presented the $M(H)$ loops at high-T_a's, for both the cases of t_{Ag}, t_{Cu} = 6 nm and t_{Ag}, t_{Cu} = 12 nm, show that a more perpendicular tendency at 400°C than at 300°C. It can indicate a more prominent FM-type alignment, as seen if comparing Fig.2c,f
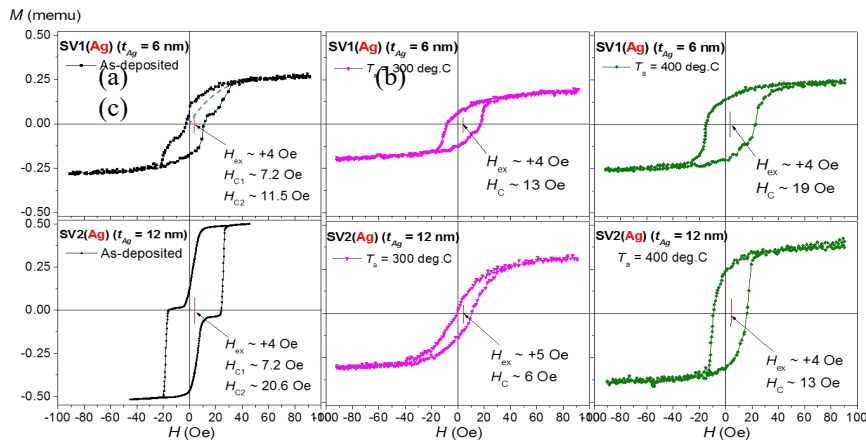
Fig. 2. $M(H)$ loops with H_C and H_{ex} for the MnNi/Co/Ag(t_{Ag})/Py SV systems annealed at T_a = 300°C and 400°C for 30 mins. (a)-(c) SV1 with t_{Ag} = 6 nm, (d)-(f) SV2 with t_{Ag} = 12 nm.
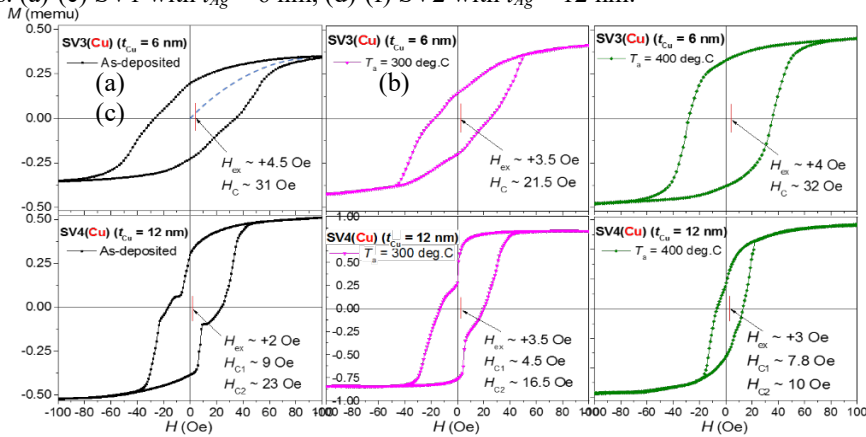
Fig. 3. $M(H)$ loops with H_C and H_{ex} for the MnNi/Co/Cu (t_{Cu})/Py SV systems annealed at T_a = 300°C and 400°C for 30 mins. (a)-(c) SV3 with t_{Cu} = 6 nm, (d)-(f) SV4 with t_{Cu} = 12 nm.
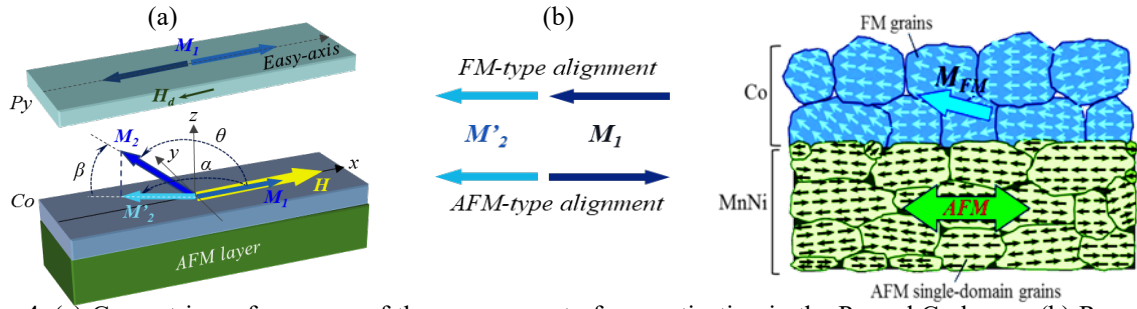
Fig. 4. (a) Geometric performances of the arrangement of magnetization in the Py and Co layers. (b) Representation of the FM- and AFM-type alignments in the SVs. (c) Depiction of a tilted-type grain morphology (out-of-plane anisotropic) in the Co layer and a multi-domain (or grain-type) structure in the NiMn layer.

versus b, e, respectively, for the cases of the NM = Ag, and comparing Fig.3c versus b for the case of the NM = Cu with only t_{Cu} = 6 nm. Whereas this rule seems invalid for the case of t_{Cu} = 12 nm (compare Fig.3f versus e). Another effect of T_a on magnetic properties is just a substantial enhancement of H_C when the SVs were annealed at the high-T_a's. Fig.2 and 3 show an increase in H_C and in the slope of the related $M(H)$ loop with increasing T_a (compare the loops between T_a = 300ºC and 400ºC). This can be a consequent of magneto-crystalline anisotropy, characterized by an effective K_u/M_S ratio, and of an exchange-bias coupling (EBC) between the NiMn and Co layers with an exchange-biased field H_{ex}, as will be mentioned below.

Lastly, an EBC phenomenon induced by the NiMn/Co interfaces has been observed for both the SV systems. The SVs have a positive shift tendency, as indicated in Fig.2 and 3, and the exchange-biased field H_{ex} received for these SVs are quite small, H_{ex} ~ +(2÷5) Oe. The weak in-plane H_{ex}'s can be explained since no-field cooling after annealing of the SVs, because we expect that the exchange bias can be obtained and the H_{ex} can be controlled without a cooling field, as suggested in Refs.[16,17]. This is an opportunity to tune the exchange bias even just after device fabrication [16]. On the other hand, the high T_a can result in a deviation in chemical stoichiometry of the MnNi alloy, as well as a destruction of the MnNi/Co interfaces, as pointed out [18]. Positive EBC behaviors often are observed in many FM/AFM bilayer systems where H is directed away from the direction of the anisotropic axis or the sample plane [19-20]. Such behaviors can prove that there was an effective out-of-plane anisotropy in the SVs, as illustrated in Fig.4a for the case of M_2 corresponding with $\alpha > 90°$. A interlayer exchange coupling (IEC) energy of FM layers can be expressed as $E_{ex} = -j_1[M_1 M_2/(|M_1|.|M_2|)] - j_1[M_1 M_2/(|M_1|.|M_2|)]^2 = -j_1\cos(\theta) - j_2\cos^2(\theta)$, there θ (Fig.4a) is the angle between M_1 and M_2 [20]. For the first term, j_1 represents the bilinear coupling described the FM and AFM coupling corresponding to $\theta = 0°$ and 180°. For the second term, j_2 describes the biquadratic coupling corresponding to

θ = 90°. In the case of the weak out-of-plane anisotropy, β ~0 and α ~0 or ~180°, M_2 is replaced by M_2' and a configuration as exhibited in Fig.4b was used to indicate the FM- and AFM-type alignments. Therefore, j_2 of biquadratic coupling can be neglected, $E_{ex} \approx -j_1\cos(\alpha) \approx -j_1 = j/(2A)$, where j is the IEC constant per interface area A determined by the difference in energy between FM and AFM configurations: $j = (E_{AFM} - E_{FM})/(2A)$ [8]. Note that j is very small because of weak-E_{AFM} and -E_{FM}, leading to the E_{ex} is low in the SVs. As a result, the in-plane unidirectional anisotropy constant $J_K \equiv M_s d_{Co} H_{ex}$, where M_s and d_{Co} is saturation magnetization and thickness of the Co layer, respectively, is quite small due to the quite weak H_{ex}. That is why there is an out-of-plane anisotropy in the SVs studied here. On the other side, as has been pointed out by another work that, apart from the perpendicular anisotropy of the Co layer can induce an interlayer perpendicular exchange coupling between the Co and NiMn layers for a thicker-AFM thickness, such as d_{NiMn} = 25 nm in this study. This implies that a perpendicular EBC, which can be used to explain on the double-shifted phenomenon for the SVs, was induced slightly by a perpendicular-type spin exchange coupling morphology at the NiMn/Co interfaces. Moreover, the two-step-like features observed in some $M(H)$ loops, as seen in Fig.2 and 3, can also indicate a contribution of a double-shifted phenomenon. Because this double-shifted effect is usually occured when the AFM/FM junctions is either zero-field cooled in a demagnetized state or grown in zero field. This is due to an imprint of the domain pattern of the FM into the AFM during the cooling procedure after annealing [21], as executed for our SVs in this study. Consequently, for the SVs annealed at high-T_a's such as at 300ºC and 400ºC, a distribution in blocking temperature T_B of NiMn layer can be caused by the distribution in grain-sizes, stoichio-metry, strains, or defects in the layers [21,22]. Thus, at the FM/AFM interface, there can be a grain configuration with unequal numbers of parallel and antiparallel spins at the surface of the grains, due to grain size, shape, or roughness [23]. Those results

suggest about a nonuniform distribution of spin direction at the interfaces, for which a tilted spin configuration at around the FM/AFM interfaces is implied, and the spin canting out of plane plays an important role in the origin of the perpendicular EBC [24]. Then a fine grain-like morphology should be prominent in the NiMn and Co layers, so that M_{FM} (or M_2) of the Co grains almost is out-of-plane, but a general AFM easy-axes of all the NiMn single-domain grains maintains almost in-plane, as sketched in Fig.4c.

4. Conclusion

Magnetization process and magnetic coupling in the NiMn/Co/Ag(Cu)/Py SVs annealed at high-T_a's ($300^{\circ}C$ and $400^{\circ}C$) reveal some salient points as follow: (*i*) These SV systems have a quite weak magnetic interaction between Co and Py layers. (*ii*) There is clearly a feature of magnetic anisotropic behavior tilted away from the plane – out-of-plane magnetic anisotropy, which is attributed mainly to magnetic surface anisotropy of the Co layer. (*iii*) There is a weak bias in the positive exchange bias coupling between NiMn and Co layers, which is thought to be originated from the out-of-plane anisotropy of the Co layer and from the morphology of a multi-domain AFM structure in NiMn layer.

Acknowledgments

References

[1] B. Dieny, et al., Giant magnetoresistance in soft ferromagnetic multilayers, Phys. Rev. B 43 (1991) 1297–1300.

[2] P.A. Grünberg, Nobel Lecture: From spin waves to giant magnetoresistance and beyond. Rev. Mod. Phys. 80 (2008) 1531-1540.

[3] A. Fert, Nobel lecture: Origin, development, and future of spintronics. Rev. Mod. Phys. 80 (2008) 1517-1530.

[4] A. Guedes, et al., Hybrid GMR Sensor Detecting 950 pT/sqrt(Hz) at 1 Hz and Room Temperature, Sensors 18 (2018) 790 (8 ps).

[5] L. Jogschies, et al., Recent Developments of Magnetoresistive Sensors for Industrial Applications, Sensors 15 (2015) 28665-28689.

[6] T. Shinjo, Ch.1- Experiments of Giant Magneto-resistance, in Spin Dependent Transport in Magnetic Nanostructures, Eds. by S. Maekawa and T. Shinjo, CRC Press (LLC), Boca Raton – London – New York – Washington, D.C., 2002.

[7] S.S.P. Parkin, R. Bhadra, K.P. Roche, Oscillatory Magnetic Exchange Coupling through Thin Copper Layers, Phys. Rev. Lett. 66 (1991) 2152-2155.

[8] C.-H. Chang, et al., Engineering the interlayer exchange coupling in magnetic trilayers; Sci. Rep. 5 (2015) 16844.

[9] A. Gayen, et al., Interlayer coupling in symmetric and asymmetric CoFeB based trilayer films with different domain structures: Role of spacer layer and temperature, J. Magn. Magn. Mater. 462 (2018) 29-40.

[10] C.-G Lee, et al., Effects of annealing on the GMR and domain structure stabilization in a Py/Cu/Py/MnIr spin valve, J. Magn. Magn. Mater. 272-276 (2004) 1887-1888.

[11] C. Chappert, P. Bruno; Magnetic anisotropy in metallic ultrathin films and related experiments on cobalt films, J. Appl. Phys. 64 (1988) 5736-5741.

[12] P. Bruno, J.-P. Renard; Magnetic Surface Anisotropy of Transition Metal Ultrathin Films, Appl. Phys. A 49 (1989) 499-506.

[13] P. Bruno, et al.; Magnetic hysteresis of cobalt ultrathin films with perpendicular anisotropy, J. Magn. Magn. Mater. 93 (1991) 605-608.

[14] Nguyen Anh Tuan, et al., Inverse MR and Dual-AMR Phenomena in Co/CoO/Ag/Co Sandwiches, J. Kore. Phys. Soc. 72 (2018) 786-794.

[15] F.J. Rachford, et al.; Magnetization and FMR studies of crystal-ion-sliced narrow linewidth gallium-doped yttrium iron garnet, J. Appl. Phys. 87 (2000) 6253-6255.

[16] P. Miltenyi et al., Tuning exchange bias, Appl. Phys. Lett. 75 (1999) 2304-2306.

[17] J. Sort, et al., Exchange bias effects in Fe nanoparticles embedded in an antiferromagnetic Cr_2O_3 matrix, Nanotechnology 15 (2004) S211-S214.

[18] H.W. Chang, et al., Exchange bias in Co/MnPt polycrystalline films on Si(100)/SiO_2 substrates with Ta underlayer, Thin Solid Films 660 (2018) 834-839.

[19] L. Sun, P. C. Searson, C. L. Chien, Asymmetrical hysteresis in exchange-biased multilayers with out-of-plane applied fields, Phys. Rev. B 71 (2005) 012417.

[20] D.E. Burgler, S.O. Demokkritov, P. Grunberg, M.T. Johnson, Ch.1: Interlayer exchange coupling in layered magnetic structures in Handbook of Magnetic Materials, Volume 13, 1st Edition, Ed. by K.H.J. Buschow, North Holland, Elsevier, 2001, 1-85.

[21] S. Brück, et al., Exploiting Length Scales of Exchange-Bias Systems to Fully Tailor Double-Shifted Hysteresis Loops, Adv. Mater. 17 (2005) 2978-2983.

[22] J.-V. Kim, et al., Angular dependence and interfacial roughness in exchange-biased ferromagnetic/anti-ferromagnetic bilayers, Phys. Rev. B 61 (2000) 8888-8894.

[23] A.E. Berkowitz, K. Takano, Exchange anisotropy – A review, J. Magn. Magn. Mater. 200 (1999) 552-570.

[24] N.N. Phuoc, T. Suzuki; Perpendicular exchange bias mechanism in FePt/FeMn multilayers, J. Appl. Phys. 101 (2007) 09E501.